Applied Physics Letters ARTICLE scitation.org/journal/apl

Origami-equivalent compliant mechanism

Cite as: Appl. Phys. Lett. **115**, 171904 (2019); doi: 10.1063/1.5115790
Submitted: 19 June 2019 · Accepted: 14 October 2019 ·
Published Online: 23 October 2019

Soroush Kamrava,[1] Ranajay Ghosh,[2] Jian Xiong,[3] Samuel M. Felton,[1] and Ashkan Vaziri[1,a)]

AFFILIATIONS

[1]Department of Mechanical and Industrial Engineering, Northeastern University, Boston, Massachusetts 02115, USA
[2]Department of Mechanical and Aerospace Engineering, University of Central Florida, Orlando, Florida 32816, USA
[3]Center for Composite Materials and Structures, Harbin Institute of Technology, Harbin 150001, People's Republic of China

[a)]Author to whom correspondence should be addressed: vaziri@coe.neu.edu

ABSTRACT

Origami structures have gained tremendous attention due to their extreme kinematic performance. However, typical origami structures suffer from poor load-bearing capacity due to extreme slenderness of facets. In this letter, we introduce a technique to design an origami-equivalent compliant mechanism which preserves the origami kinetics and kinematics while offering higher load-bearing capacity compared to the original origami structure. In this technique, we offer an energy equivalence principle between the origami and the compliant mechanism. We validate the principle using experimental investigation for a square-twist origami pattern. This principle thus opens up a significant avenue for designing deployable and programmable structures.

Origami structures, consisting of segmented flat facets, can be fully described through straightforward mathematical relationships. This makes the origami a reliable paradigm for building various structures with a wide range of functionalities.[1,2] For instance, origami-based structures have been made with intriguing properties such as programmable auxeticity,[3–5] self-folding,[1,6–10] reconfigurability,[11–14] bistability and multistability,[15–17] vibration isolation,[18,19] and tunable stiffness.[20,21] Expansion of these features or creating new functionalities in the origami structures requires a full understanding of their behavior which has been done through different modeling approaches.[22,23] Traditional modeling approaches need to be modified to incorporate facet deformation[22,24–26] which is especially inevitable due to their slender structures. Facet deformation can itself be a reason for emerging new properties in the origami structures, for instance, bistability.[15,17] Such properties made the origami-based systems a potential candidate for applications in various engineering purposes such as deployable solar panels,[27] medical stents,[28] robotic manipulators,[29,30] and fold-core sandwich panels,[31] as well as functional load-bearing systems.[32]

Although using the extremely thin facets in making origami structures results in the straightforward kinematic analysis, the thin facets undermine their load-bearing capacity. Using thicker face sheets prevents utilizing the full range of origami kinematics[33,34] thereby defeating the purpose. In this letter, we propose an alternative approach for increasing the load-bearing capacity of origami structures where we substitute the origami facets with either rigid or deformable linkages while preserving the essential kinematic and kinetic performance. Such deformable mechanisms are called compliant mechanisms, which are a set of interconnected linkages which can elastically deform under certain loadings to achieve a desired set of movements.[35,36] The connection between complaint mechanism and origami pattern has been studied in the literature from different perspectives.[37–40] For example, Greenberg *et al.* proposed a method based on graph theory to investigate the coupling between the behavior of origami structures and compliant mechanisms.[24] Also, Filipov *et al.* proposed a method in which the deformable facets of origami can be replaced with bars, hinges, and springs to form a mechanism with similar properties to the original origami structure.[23] Here, we develop a practical method based on the numerical analysis to come up with a compliant mechanism design which mimics both the kinematics and kinetics of the original origami structure. We hypothesize that an equivalence in performance can be achieved using a strain energy equivalence principle between the origami and the compliant mechanism. The equivalence would mean reproducing the original kinematics (the way it folds) and kinetics (the forces required for folding) of the origami. We apply this hypothesis to a square-twist origami, which consists of an inner-square facet located at the center, four identical trapezoidal facets, and four identical rectangular facets located at the corners, see Fig. 1(a). The square-twist is also a deformable origami, in which all three facet types (inner-square, trapezoidal, and rectangular) deform during the folding procedure, see Fig. 1(b). Each square-twist pattern can be fully defined using three independent geometrical

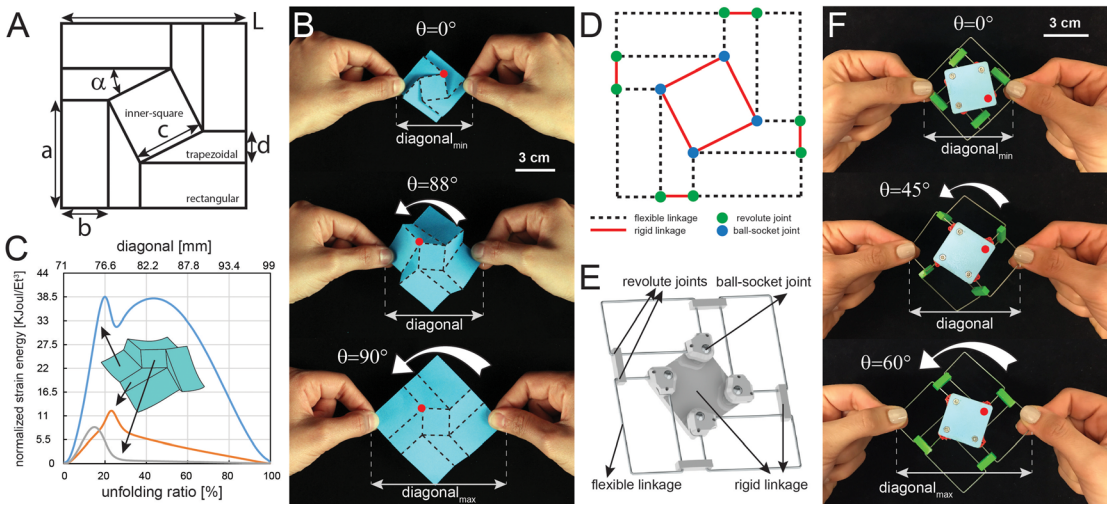

FIG. 1. (a) Crease pattern and geometrical parameters of the square-twist origami. (b) Unfolding of a square-twist origami through applying in-plane tension along its diagonal line. (c) Normalized strain energy stored in different facet types (obtained from finite element simulation) vs unfolding ratio (lower axis). (d) Dashed lines represent members with dominant energy and solid lines represent low energy members. The connection between linkages is shown with circular markers and is assigned to be revolute or ball-socket joints based on their desired motion in the original origami structure. (e) The energy dominant members are fabricated using a deformable steel wire and remaining are 3D printed as thick and rigid members to mimic the behavior of the paper origami. (f) Unfolding of a compliant mechanism with similar folding/unfolding characteristics as a square-twist paper origami.

parameters L, c, and α, where L is the side length of the outer-square in origami pattern, c is the side length of the inner-square, and α is one of the nonright internal angles of the trapezius, see Fig. 1(a). All other geometrical parameters of the square-twist pattern can be determined using Eqs. (1)–(3),

$$a = \frac{L}{2} - \frac{c}{2}(\sin\alpha - \cos\alpha), \tag{1}$$

$$b = \frac{L}{2} - \frac{c}{2}(\sin\alpha + \cos\alpha), \tag{2}$$

$$d = c\sin\alpha. \tag{3}$$

Figure 1(b) shows unfolding of a square-twist origami with $L = 70$ mm, $\alpha = 45°$, and $c = 20$ mm through applying in-plane tension along its diagonal, which causes the inner square to rotate by $\theta°$. The stored strain energy differs in different facet types (inner-square, trapezoidal, and rectangular) but it is identical for the same facets type because of symmetry in the pattern. We model the unfolding of the square-twist origami with $L = 70$ mm and $\alpha = 30°$ using finite element (FE) simulation. The boundary conditions are imposed, which move all four corners of the outer-square outward along the diagonals while keeping them fixed in the out-of-plane direction. Figure 1(c) shows the value of strain energy stored in the three facet types, inner-square, rectangular, and trapezoidal, as a function of unfolding percentage defined as $100 \times \left(\frac{\text{diagonal} - \text{diagonal}_{\min}}{\text{diagonal}_{\max} - \text{diagonal}_{\min}}\right)$, where diagonal is the instantaneous distance between two nonadjacent corners of outer-square in square-twist origami at any level of folding and $\text{diagonal}_{\max}$ and $\text{diagonal}_{\min}$ are the maximum and minimum values of the diagonal, respectively [see Fig. 1(b)]. The plot shows that the stored energy in rectangular facets dominates other members, which are minor and considered low-energy members.

We now propose an energy-equivalent origami design through assigning rigid and deformable linkages to low-energy and dominant-energy members. We replace each rectangular facet (dominant in energy) with a deformable rectangular frame representing the facet edges. The frame retrieves the elastic response to in-plane tension/compression, shear, and bending loadings, which are the fundamental loading modes in an origami structure.[23] Then, we replace all edges of the inner-square and trapezoidal facets (low in energy), with rigid linkages except those are shared between the rectangular and trapezoidal facets and already assigned as a dominant elastic energy member. Note that the inner-square facet can be replaced with a rigid square member since all of its edges are assigned to be rigid. Figure 1(d) shows the composition of different linkages where dashed lines and solid lines are the flexible and rigid linkages, respectively. Using this construction, we ensure that all the elastic energy from deformation would come from the flexible linkages. The connection points [shown with circular markers in Fig. 1(d)] are assigned to be either revolute or ball-socket joints based on their desired motion in the original square-twist origami pattern. Figure 1(e) shows a graphical illustration of the fabricated proposed compliant mechanism where the energy dominant linkages are fabricated using a deformable steel wire with a diameter of 0.81 mm and low-energy members are 3D printed as thick and rigid linkages. The inner-square facet is replaced with a 3D printed rigid square plate. The ball-socket and revolute joints are also shown in this figure.

Figure 1(f) confirms that the unfolding of compliant mechanism is similar to the square-twist origami pattern. Unfolding of both paper origami and the proposed compliant mechanism can be quantified using the rotation value of inner-square, $\theta°$. Note that θ for an ideal thin square-twist origami (zero-thickness facets) is

$$\theta = \begin{cases} 2\alpha, & 0 < \alpha < 45^\circ \\ 2(\alpha - 180^\circ), & 135^\circ < \alpha < 180^\circ. \end{cases} \quad (4)$$

See the supplementary material for derivation of Eq. (4). However, for an origami made from thick paper (nonzero thickness) or equivalent compliant mechanism, $\theta = 2\alpha - \delta$ (or $2\alpha - 360^\circ - \delta$) where δ is the offset from the zero-thickness origami due to the internal contact between members. The square-twist origami patterns with $45^\circ < \alpha < 135^\circ$ are excluded from consideration since they cannot achieve the fully folded configuration due to inherent geometrical limitations even for zero-thickness members.

We now compare the performance of the original origami and its equivalent compliant mechanism. Figure 2(a) shows the front view of the unfolded and folded square-twist compliant mechanism where the inner-square plate and the rigid linkages are colored in blue and green, respectively. The geometrical parameters that describe the geometry of the mechanism are shown in Fig. 2(a). We choose the rotation of inner-square (θ) and extension in diagonal direction as two geometrical parameters describing the overall configuration of origami and quantify

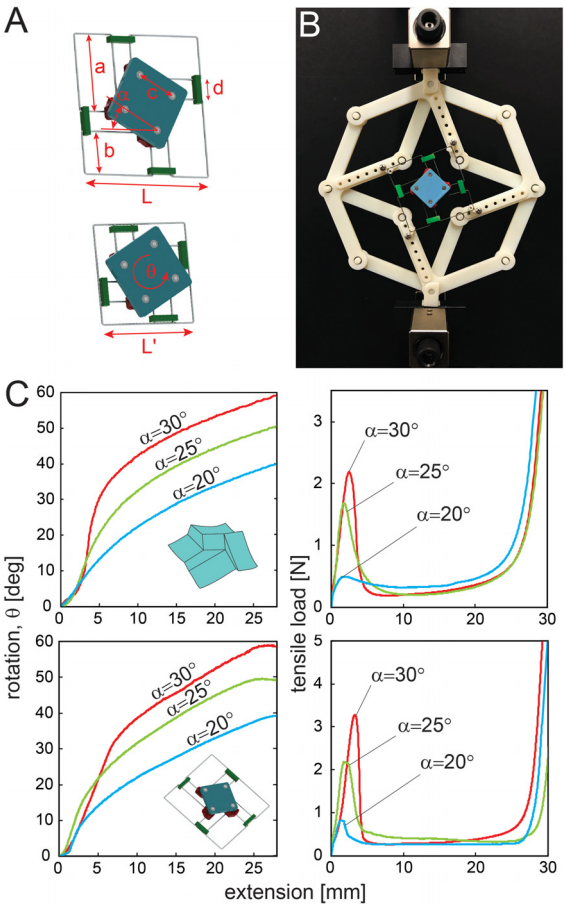

FIG. 2. (a) Unfolded and folded configurations of the equivalent compliant mechanism. (b) Biaxial tensile test on the proposed compliant mechanism and paper origami (not shown here). (c) The rotation of the inner square (θ) and the applied tensile load along the diagonal lines vs the diagonal extension measured experimentally for three paper origamis and three equivalent compliant mechanisms.

the kinematics of folding using the change of θ as a function of diagonal extension. The kinetics of folding can be quantified using the forces required to fold or unfold the origami/mechanism, which would be the applied bidirectional compression or tension along the diagonals.

We fabricated three paper origami and three origami-based complaint mechanism prototypes with ($L = 70$ mm, $\alpha = 30^\circ$, and $c = 20$ mm), ($L = 70$ mm, $\alpha = 25^\circ$, and $c = 23.7$ mm), and ($L = 70$ mm, $\alpha = 20^\circ$, and $c = 29.2$ mm). Because of the existing asymmetry in the square-twist pattern, a bidirectional tensile test is preferred, which causes identical deformed shape in facets from the same type during the folding or unfolding process. The biaxial tensile test is performed using a single-column Instron 5582 testing machine in conjunction with a 3D printed customized testing mechanism, which transfers the load and displacement applied from the testing machine equally to both orthogonal diagonal directions, see Fig. 2(b) and the supplementary material for detailed information regarding the testing mechanism. Figure 2(c) shows plots of bidirectional tensile load and rotation of inner-square (θ) vs diagonal extension for all six tested prototypes. The rotation of inner-square in both paper origami and the compliant mechanism starts from the zero at zero diagonal extension and goes to the maximum rotation value of $2\alpha - \delta$ at maximum diagonal extension of $20\sqrt{2}$ mm. Maximum diagonal extension is a function of angle α and can be determined from subtracting the diagonal length of origami in the folded configuration from the unfolded configuration,

$$\text{Maximum diagonal extension} = \text{diagonal}_{\max} - \text{diagonal}_{\min} = 2\sqrt{2}\,c\sin\alpha. \quad (5)$$

Our plots show that both the compliant mechanism and origami exhibit similar profiles of gradually decreasing slope and range of diagonal extension. These similarities are even stronger for the kinetic tests as seen in Fig. 2(c) (right), which show a rapid increase and decrease in the initial values of tensile load and bistability in all six samples.[15] The bistability seen in the original origami is also reproduced in the proposed origami equivalent structure and is a direct consequence of energy equivalence. Note that in spite of these similarities in force-displacement diagrams, the force magnitudes are different but are expected due to using different materials for fabricating them and we believe that the force magnitude is a direct function of the geometry and material properties of the metal wire. All the results presented in Fig. 2 are extracted from the experimental testing using the Instron machine and a customized biaxial testing setup, please see the supplementary material for more information on the reproducibility of the results.

The square-twist complaint mechanism can be used to create a variety of multifunctional structures. Specifically, creating 3D shapes is of great interest for designing deployable structures. We will now compare the relative behavior of 3D structures made using the compliant mechanism and original origami. We fabricate a 3D inflatable rotational cube made of the proposed compliant mechanism and compare its load-displacement characteristic with the equivalent origami structure. The cube is made by assembling a six square-twist mechanism into a cubic shape (each mechanism serves as one face of the cube), see Fig. 3(a) (Multimedia view). Note that the inner-square is fabricated in a round shape to make all facets alike although they have different c values. In the next step, putting a balloon inside the assembled

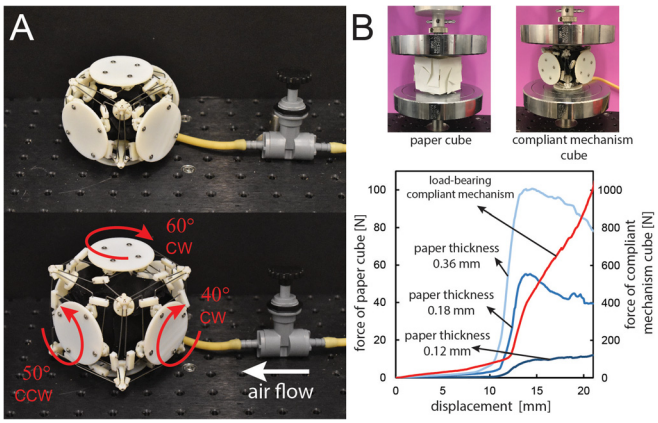

FIG. 3. (a) A load-bearing origami-based cube consisting of six square-twist compliant mechanisms that are assembled to make a cubic shape. (b) Comparison of load-bearing capacity between paper cubes made out of three different paper type and the proposed compliant mechanism cube. Multimedia view: https://doi.org/10.1063/1.5115790.1

cube provides the single source of actuation for the rotational cube where pressurizing the balloon opens all faces simultaneously and results in potentially six different rotations at different faces, see Fig. 3(a) and supplementary Movie. This cube can be used as an actuator which provides different amounts of rotation values at different faces using a single source of actuation. The demonstrated rotational cube in Fig. 3(a) is designed and fabricated in a way that pressurizing the balloon causes 60° CW, 50° CCW, 40° CW, 60° CCW, 50° CW, and 40° CCW rotations on the faces. The presented inflatable rotational cube was also made out of paper with the same folding and unfolding characteristics for comparison.

Here, we compare the load-bearing capacity of the proposed compliant mechanism cube with an ordinary paper origami cube. We fabricate six square-twist origami with $L = 70$ mm, $\alpha = 30°$, and $c = 20$ mm out of paper and glue them in a cubic form to make a paper origami cube, see Fig. 3(b). We apply an axial compression load on them and capture the load-displacement curve for each sample using a single-column Instron machine, see Fig. 3(b). The blue plots in Fig. 3(b) show the results for compression test of three paper cubes made out of papers with 0.12 mm, 0.18 mm, and 0.36 mm thicknesses (Strathmore, 500 Bristol sheets, Plate Surface). Further thickening the paper results in a limited range of folding and round creases instead of sharp creases. All samples have been compressed for 21 mm and the maximum reported load values for 0.12 mm, 0.18 mm, and 0.36 mm samples are 13, 45, and 100 N, respectively (see the left vertical axis for the load values for paper samples). The red curve shows the compression test result for the load-bearing compliant mechanism cube in which the maximum reported load value is 1044 N (see the right vertical axis for the load values for the compliant mechanism cube). The maximum load borne by the compliant mechanism cube was almost an order of magnitude greater than the thickest paper origami cube, confirming a considerable improvement in the load-bearing capacity of the proposed system, while preserving the essential kinematics and kinetics of the origami.

In conclusion, we hypothesized and validated an energy equivalent principle for the synthesis of the origami based compliant mechanism with equivalent characteristics to the square-twist origami pattern and higher load bearing capacity. Although the resultant compliant mechanism has a similar behavior to the original origami pattern, we are not able to categorize it as an origami structure since it is not made through the folding action. However, the title of "origami-equivalent compliant mechanism" can truly describe the similarities and differences between these two concepts. This process has been done through the study of paper origami to identify the contribution level of each facet in building the energy landscape of the system and replacing them with rigid or deformable components based on the obtained results. We validated our method through comparing the kinematics and kinetics of a square-twist origami with the proposed equivalent compliant mechanism. The square-twist origami has been chosen for the validation of the proposed method because of its complex kinematics of the folding and complex kinetics arising from both hinge rotation and facet deformation. We believe that equivalency between different aspects of the kinematics and kinetics of the original origami and the designed compliant mechanism validates the functionality of the proposed method and demonstrates its ability to be applied for other origami patterns. At the end, we designed and fabricated a functional inflatable rotational cube based on the proposed compliant mechanism to demonstrate the higher load-bearing capacity and potential functionalities for such an origami-inspired compliant mechanism.

See the supplementary material for more information on the square-twist origami pattern, biaxial testing, and inflatable cube design.

This work was supported by the United States National Science Foundation, Division of Civil, Mechanical, and Manufacturing Innovation, Grant No. 1634560.

REFERENCES

[1]S. Felton, M. Tolley, E. Demaine, D. Rus, and R. Wood, Science **345**, 644 (2014).
[2]S. Li, D. M. Vogt, D. Rus, and R. J. Wood, Proc. Natl. Acad. Sci. **114**, 13132 (2017).
[3]S. Kamrava, D. Mousanezhad, H. Ebrahimi, R. Ghosh, and A. Vaziri, Sci. Rep. **7**, 46046 (2017).
[4]A. Rafsanjani and D. Pasini, Extreme Mech. Lett. **9**, 291 (2016).
[5]H. Yasuda and J. Yang, Phys. Rev. Lett. **114**, 185502 (2015).
[6]J. H. Na, A. A. Evans, J. Bae, M. C. Chiappelli, C. D. Santangelo, R. J. Lang, T. C. Hull, and R. C. Hayward, Adv. Mater. **27**, 79 (2015).
[7]M. T. Tolley, S. M. Felton, S. Miyashita, D. Aukes, D. Rus, and R. J. Wood, Smart Mater. Struct. **23**, 094006 (2014).
[8]G. J. Hayes, Y. Liu, J. Genzer, G. Lazzi, and M. D. Dickey, IEEE Trans. Antennas Propag. **62**, 5416 (2014).
[9]V. B. Shenoy and D. H. Gracias, MRS Bull. **37**, 847 (2012).
[10]J.-S. Koh, S.-R. Kim, and K.-J. Cho, in *ASME 2014 International Design Engineering Technical Conferences and Computers and Information in Engineering Conference* (American Society of Mechanical Engineers, 2014), p. V05BT08A043.
[11]J. T. Overvelde, T. A. De Jong, Y. Shevchenko, S. A. Becerra, G. M. Whitesides, J. C. Weaver, C. Hoberman, and K. Bertoldi, Nat. Commun. **7**, 10929 (2016).
[12]S. Yao, X. Liu, S. V. Georgakopoulos, and M. M. Tentzeris, in *2014 IEEE Antennas and Propagation Society International Symposium (APSURSI)* (IEEE, 2014), p. 374.
[13]D. Mousanezhad, S. Kamrava, and A. Vaziri, Sci. Rep. **7**, 14792 (2017).
[14]S. Kamrava, R. Ghosh, Y. Yang, and A. Vaziri, Europhys. Lett. **124**, 58001 (2018).
[15]J. L. Silverberg, J.-H. Na, A. A. Evans, B. Liu, T. C. Hull, C. D. Santangelo, R. J. Lang, R. C. Hayward, and I. Cohen, Nat. Mater. **14**, 389 (2015).

[16]A. Pagano, B. Leung, B. Chien, T. Yan, A. Wissa, and S. Tawfick, in *ASME 2016 Conference on Smart Materials, Adaptive Structures and Intelligent Systems* (American Society of Mechanical Engineers, 2016), p. V002T06A005.
[17]S. Kamrava, R. Ghosh, Z. Wang, and A. Vaziri, Adv. Eng. Mater. **21**, 1800895 (2019).
[18]S. Sadeghi and S. Li, Smart Mater. Struct. **28**, 065006 (2019).
[19]S. Ishida, K. Suzuki, and H. Shimosaka, J. Vib. Acoust. **139**, 051004 (2017).
[20]J. L. Silverberg, A. A. Evans, L. McLeod, R. C. Hayward, T. Hull, C. D. Santangelo, and I. Cohen, Science **345**, 647 (2014).
[21]S. Li, H. Fang, S. Sadeghi, P. Bhovad, and K. W. Wang, Adv. Mater. **31**, 1805282 (2019).
[22]E. A. P. Hernandez, D. J. Hartl, E. Akleman, and D. C. Lagoudas, Comput.-Aided Des. **78**, 93 (2016).
[23]E. Filipov, K. Liu, T. Tachi, M. Schenk, and G. Paulino, Int. J. Solids Struct. **124**, 26 (2017).
[24]H. Greenberg, M. L. Gong, S. P. Magleby, and L. L. Howell, Mech. Sci. **2**, 217 (2011).
[25]L. A. Bowen, C. L. Grames, S. P. Magleby, L. L. Howell, and R. J. Lang, J. Mech. Des. **135**, 111008 (2013).
[26]L. A. Bowen, C. L. Grames, S. P. Magleby, R. J. Lang, and L. L. Howell, in *ASME 2013 International Design Engineering Technical Conferences and Computers and Information in Engineering Conference* (American Society of Mechanical Engineers, 2013), p. V06BT07A044.
[27]S. A. Zirbel, R. J. Lang, M. W. Thomson, D. A. Sigel, P. E. Walkemeyer, B. P. Trease, S. P. Magleby, and L. L. Howell, J. Mech. Des. **135**, 111005 (2013).
[28]K. Kuribayashi, K. Tsuchiya, Z. You, D. Tomus, M. Umemoto, T. Ito, and M. Sasaki, Mater. Sci. Eng. A **419**, 131 (2006).
[29]S. Kamrava, D. Mousanezhad, S. M. Felton, and A. Vaziri, Adv. Mater. Technol. **3**(3), 1700276 (2018).
[30]B. J. Edmondson, L. A. Bowen, C. L. Grames, S. P. Magleby, L. L. Howell, and T. C. Bateman, in *ASME 2013 Conference on Smart Materials, Adaptive Structures and Intelligent Systems* (American Society of Mechanical Engineers, 2013), p. V001T01A027.
[31]S. Heimbs, *Dynamic Failure of Composite and Sandwich Structures* (Springer, 2013), p. 491.
[32]C. Lv, D. Krishnaraju, G. Konjevod, H. Yu, and H. Jiang, Sci. Rep. **4**, 5979 (2014).
[33]R. J. Lang, K. A. Tolman, E. B. Crampton, S. P. Magleby, and L. L. Howell, Appl. Mech. Rev. **70**, 010805 (2018).
[34]Y. Chen, R. Peng, and Z. You, Science **349**, 396 (2015).
[35]M. L. Culpepper and G. Anderson, Precis. Eng. **28**, 469 (2004).
[36]Y. Tian, B. Shirinzadeh, D. Zhang, and Y. Zhong, Precis. Eng. **34**, 92 (2010).
[37]L. A. Shaw, S. Chizari, M. Dotson, Y. Song, and J. B. Hopkins, Nat. Commun. **9**, 4594 (2018).
[38]K. Francis, J. Blanch, S. Magleby, and L. Howell, Mech. Sci. **4**, 371 (2013).
[39]I. L. Delimont, S. P. Magleby, and L. L. Howell, J. Mech. Rob. **7**, 011009 (2015).
[40]B. J. Edmondson, L. A. Bowen, C. L. Grames, S. P. Magleby, L. L. Howell, and T. C. Bateman, in *ASME 2013 Conference on Smart Materials, Adaptive Structures and Intelligent Systems* (American Society of Mechanical Engineers Digital Collection, 2014).